Global Deficiency of Chaperone-Mediated Autophagy Leads to Low Cancellous Bone Mass in Young Adult Mice

Nisreen Akel, Milena Dimori, Ryan S. Macleod, Stuart B. Berryhill, Julie A. Crawford, and Melda Onal

University of Arkansas for Medical Sciences, AR, USA

ASBMR® 2020 Annual Meeting

September 11–15, 2020

Virtual Event

INTRODUCTION

Based on the delivery mechanisms utilized to transfer the targets to the lysosomes, autophagy is separated into three types: macroautophagy, chaperone-mediated autophagy, and microautophagy. We have previously shown that macroautophagy in osteoblast lineage is essential for skeletal health[1,2]. However, whether other types of autophagy are relevant in bone, or what physiological/pathophysiological role they play in bone cells is unknown. **Our goal is to start assessing the role of chaperone-mediated autophagy for skeletal health under physiological and pathophysiological conditions.**

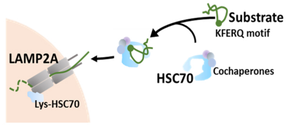

Fig 1. Chaperone-mediated autophagy illustration

In CMA, selective protein cargo is recognized by a cytosolic chaperone (HSC70), unfolded and transferred into the lysosomes one by one, by a translocation complex composed of a LAMP2A multimer at the lysosomal membrane.

Chaperone-mediated Autophagy (CMA)[3]:

- can eliminate soluble cytoplasmic proteins that are damaged, incorrectly folded, or targeted for selective proteome remodeling.
- contributes to DNA repair, cellular reprograming and cellular stress response.

METHOD

- LAMP2A is a lysosomal transmembrane protein that forms the CMA translocation complex to internalize the CMA substrates into lysosomes.
- *Lamp2a* is one of three isoforms encoded by the *Lamp2* gene and it is the isoform that is necessary to perform CMA.
- We used CRISPR/Cas9 to delete *Lamp2a* from the mouse genome, thereby producing the CMA-deficient mice.

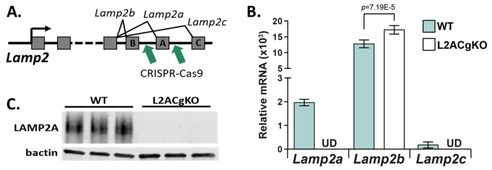

Fig 2. Production of CMA-deficient mice

A. Diagram of *Lamp2* loci showing the alternative splice sites corresponding to the three isoforms translated from the *Lamp2* gene. **B.** Real time PCR (RT-PCR) analysis of *Lamp2* isoforms in global knockout (L2ACgKO) and wild type (WT) bones showing that CRISPR-Cas9 deleted both *Lamp2a* and *Lamp2c* isoforms. Values are indicated as mean ± standard deviation (STD), n=8 mice/group, UD = undetectable. **C.** Western blot analysis of LAMP2A protein in bone lysates of L2ACgKO and WT control mice. n=3 mice/group.

RESULTS

Fig 3. Five-week-old CMA-deficient female, but not male, mice exhibit a low bone mass phenotype

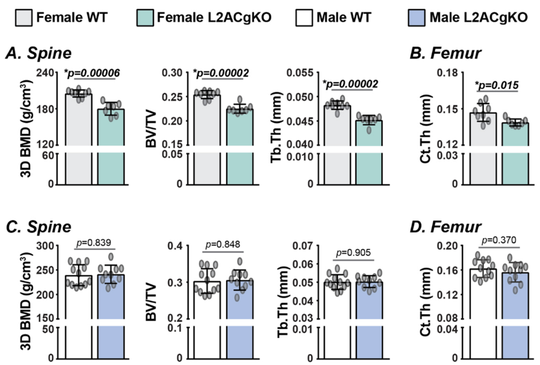

µCt analysis is performed on bones of five-week-old male and female Lamp2AC global knock-out (L2ACgKO) mice and their wild type (WT) littermates (**A-D**). Cancellous bone mass and architecture is analyzed as 3D bone mineral density (BMD), bone volume over tissue volume (BV/TV) and trabecular thickness (Tb.Th) in lumbar vertebrae 4 (**A & C**). Cortical thickness (Ct.Th) is measured at femoral midshaft (**B & D**) . n= 7-12 mice/group. Bars indicate mean ± STD. *p* values are calculated and evaluated by student's *t*-test, *, p<0.05.

Fig 4. CMA-deficient female mice have increased osteoclast marker gene and RANKL expression

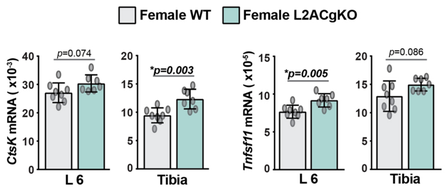

Real-time PCR (RT-PCR analysis) is used to measure mRNA levels of an osteoclast marker gene *Cathepsin K* (*CtsK*) and pro-resorptive cytokine RANKL (*Tnfsf11*) in lumbar vertebrae 6 (L6) and tibias of five-week-old female Lamp2AC global knock-out (L2ACgKO) mice and their age-matched controls (wild type mice, WT). n= 7-8 mice/group. Bars indicate mean ± STD. *p* values are calculated and evaluated by student's *t*-test, *, p<0.05.

Fig 5. Eighteen-week-old male and female CMA-deficient mice have low bone mass

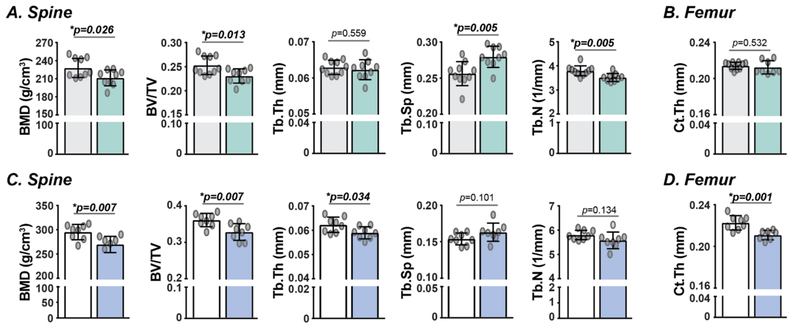

µCt analysis is performed on bones of eighteen-week-old male and female Lamp2AC global knock-out (L2ACgKO) mice and their wild type (WT) littermates (**A-D**). Cancellous bone mass and architecture is analyzed as 3D bone mineral density (BMD), bone volume over tissue volume (BV/TV), trabecular thickness (Tb.Th), trabecular separation (Tb.Sp) and trabecular number (Tb.N) in lumbar vertebrae 4 (**A & C**). Cortical thickness (Ct.Th) is measured at femoral midshaft (**B & D**) . n= 8-10 mice/group. Bars indicate mean ± STD. *p* values are calculated and evaluated by student's *t*-test, *, p<0.05.

Fig 6. CMA-deficiency is associated with increased osteoclastogenesis

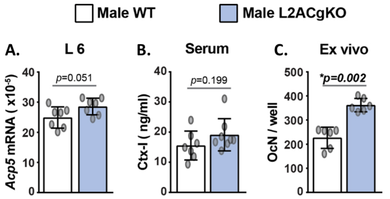

A-B, RT-PCR analysis is used to measure mRNA levels of osteoclast marker (TRAP, *Acp5*) in lumbar vertebrae 6 (L6) (**A**) and an ELISA assay is used to measure resorption marker (Ctx-I) in the serum (**B**) of eighteen-week-old male Lamp2AC global knock-out (L2ACgKO) mice and their control littermates (wild type mice, WT). n= 7-8 mice/group. **C**, Bone marrow is isolated from 4-month-old L2ACgKO and WT mice. Ex vivo adherent osteoclast formation assays are performed and osteoclast number per well (OcN/well) is quantified. n=6 wells/genotype. Bars indicate mean ± STD. *p* values are calculated and evaluated by student's *t*-test, *, p<0.05.

Fig 7. CMA-deficiency increases macroautophagy in osteoblasts

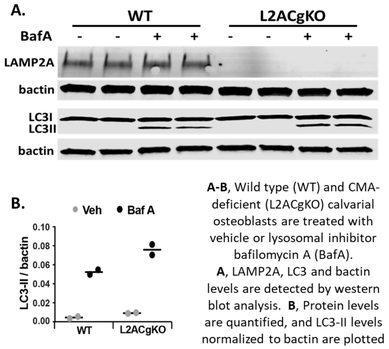

A-B, Wild type (WT) and CMA-deficient (L2ACgKO) calvarial osteoblasts are treated with vehicle or lysosomal inhibitor bafilomycin A (BafA). **A**, LAMP2A, LC3 and bactin levels are detected by western blot analysis. **B**, Protein levels are quantified, and LC3-II levels normalized to bactin are plotted to represent autophagic flux levels.

Fig 8. CMA-deficiency increases activity of ubiquitin-proteasome system in osteoblasts

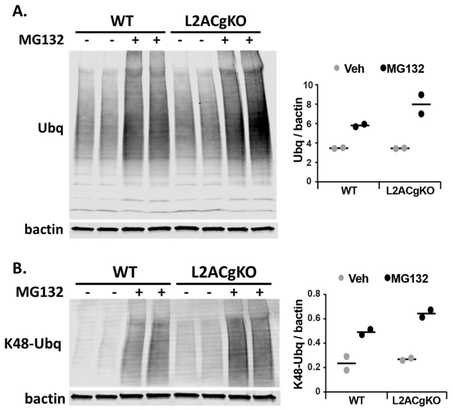

A-B, Status of the ubiquitin-proteasome system (UPS) in Wild type (WT) and CMA-deficient (L2ACgKO) calvarial osteoblasts is determined by ex vivo flux analysis using a proteasomal inhibitor (MG132). The levels of ubiquitinated proteins (**A**) and K48-linked ubiquitinated proteins (**B**), which are classical proteasome substrates, are quantified.

CONCLUSIONS

- Global elimination of CMA leads to low bone mass due to increased bone resorption.
- Elimination of CMA does not result in pronounced deficits in proteostasis possibly due to compensatory upregulation of other proteolytic pathways (macroautophagy and ubiquitin-proteasome systems).

REFERENCES

1. Onal *et al.* J Biol Chem. 2013 Suppression of autophagy in osteocytes mimics skeletal aging.
2. Piemontese *et al.* Sci Rep. 2016 Low bone mass and changes in the osteocyte network in mice lacking autophagy in the osteoblast lineage.
3. Kaushik *et al.* Nat Rev Mol Cell Biol . 2018 The coming of age of chaperone-mediated autophagy

ACKNOWLEDGEMENTS

Center for Musculoskeletal Disease Research COBRE pilot grant (P20GM125503) – supported by NIH and Bone Joint Initiative UAMS Genetic Models Core – murine model production